7  
8  
9  
10  
11  
12  
13  
14  
15  
16  
17  
18  
19

## IN\_TROD C\_TON

Textile industries discharge large amounts of colored wastewater containing various dyes (7,000,000 tons per year). Approximately 15 % of the total amount of dyes produced is lost during dyeing process and released as effluents<sup>1,2</sup>. The release of these dyes in water resources, even in small amounts, can affect aquatic life and the food web. Dyes can also cause allergic dermatitis and skin irritation and some of them have been reported to be carcinogenic and mutagenic to aquatic organisms and humans<sup>3,4</sup>. Thus, strong environmental regulations require that dye removal be performed before discharging wastewater into water bodies.

Treatment of dye effluents is difficult because these effluents are susceptible to o

61 derivatives using chemical modification techniques. Although  
 62 chitin modification products exhibit high adsorption capacity  
 63 for dyes, they are inconvenient as adsorbents in practical ap-  
 64 plications because of their relative high cost and low specific  
 65 gravity. Fungal biomass has a relatively high chitin content  
 66 ranging<sup>19,20</sup> from 10 to 90 % and is considered to be a superior  
 67 biosorbent for the removal of azo dyes<sup>21,22</sup>. However, fungi in  
 68 the form of dispersed microorganisms has a small particle size,  
 69 low density, poor mechanical strength and limited rigidity, like  
 70 most biosorbents, thus causing practical difficulties in solid-  
 71 liquid separation and biomass regeneration and limiting its  
 72 application under real conditions<sup>23,24</sup>.

73 Magnetic separation is a promising environmental purifi-  
 74 cation technique because it produces no contaminants, such  
 75 as flocculants and treats large amounts of wastewater within a  
 76 short time period of time<sup>25</sup>. Magnetic nanoparticles embed-  
 77 ded in porous polymer materials could expand the adsorption  
 78 capacity of the matrix due to enhanced electrostatic interac-  
 79 tions<sup>26</sup>. From the viewpoints of environmental protection and  
 80 resource utilization, development of novel magnetic recyclable  
 81 biomaterials, as well as exploration of their adsorption prop-  
 82 erties, is very important and significant to expand their utility  
 83 as industrial biomaterials. Recently, magnetic chitin and its  
 84 derivatives were obtained and applied in water treatment<sup>27,28</sup>.  
 85 Magnetic microbial cells, such as *Saccharomyces cerevisiae*<sup>29</sup>,  
 86 *Kluyveromyces fragilis*<sup>30</sup>, *Rhodospseudomonas spheroids*<sup>31</sup> and  
 87 so on, have also been prepared and applied in dye removal. To  
 88 the best of our knowledge, however, the characterization and  
 89 adsorption properties of magnetic fungi biomass particles for  
 90 dye removal have yet to be studied.

91 In the present study, novel magnetic *R. oryzae* biomass  
 92 particles are prepared *via* a simple method and characterized  
 93 using X-ray diffraction (XRD), scanning electron microscopy  
 94 (SEM) and Fourier transform infrared spectroscopy (FT-IR).  
 95 The effects of biosorbent dose, initial congo red concentra-  
 96 tion and contact time on the adsorption capacity of the an-  
 97 ionic azo dye congo red on magnetic *Rhizopus oryzae* biom-  
 98 ass particles are investigated. Models fitted to the equilibrium  
 99 isotherm and kinetic data are presented to validate the useful-  
 100 ness of these novel magnetic *Rhizopus oryzae* biomass par-  
 101 ticles in the treatment of practical waste effluents.

## EXPERIMENTAL

102 Congo red (molecular formula: C<sub>32</sub>H<sub>22</sub>N<sub>6</sub>Na<sub>2</sub>O<sub>6</sub>S<sub>2</sub>, molecu-  
 103 lar weight 696.66 g/mol), an anionic azo dye containing -NH<sub>2</sub>  
 104 and -SO<sub>3</sub> functional groups, was selected as a model dye (Fig. 1).  
 105 All solutions were prepared with double distilled water.

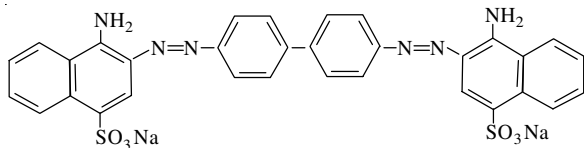


Fig. 1. Molecular structure of congo red

106 **Preparation of *R. oryzae* biomass:** The strain used was  
 107 *R. oryzae* TZ-32, a mutant of *R. oryzae* ATCC 20344. The  
 108 culture was routinely maintained at 4 °C on potato-dextrose

109 agar (PDA) and aerobically cultivated in a nutrient broth con-  
 110 taining (g/L): glucose 30, urea 2, KH<sub>2</sub>PO<sub>4</sub>0.6, MgSO<sub>4</sub>·7H<sub>2</sub>O  
 111 0.5, ZnSO<sub>4</sub>0.11 and FeSO<sub>4</sub>·7H<sub>2</sub>O 0.0088. The initial pH of the  
 112 culture was adjusted from 5.5 to 6. The spores were incubated  
 113 in a 250 mL shake flask containing 50 mL preculture medium  
 114 at 200 rev/min and 30 °C for 24 h. The fully cultured biomass  
 115 was harvested, filtered through a sieve and washed with double  
 116 distilled water. The wet biomass was dried for 24 h at 60 °C in  
 117 an oven. Dried biomass was powdered and collected for the  
 118 following experiment.

119 **Preparation of magnetic *Rhizopus oryzae* biomass par-**  
 120 **ticles:** Approximately 4.08 g of FeSO<sub>4</sub>·7H<sub>2</sub>O and 8.72 g of  
 121 FeCl<sub>3</sub>·6H<sub>2</sub>O (molar ratio of 1:2) were dissolved into 200 mL  
 122 of deoxygenated distilled water, after which 10 g of powdered  
 123 *R. oryzae* biomass was dispersed into the mixed iron salts.  
 124 Chemical precipitation was achieved at 30 °C under 0.5 h of  
 125 vigorous stirring by addition of 40 mL of NH<sub>3</sub>·H<sub>2</sub>O solution  
 126 (28 %, v/v) to the mixture in the presence of N<sub>2</sub>. The reaction  
 127 system was first heated at 40 °C for 20 min and then at 60 °C  
 128 for 2 h. The system was then cooled to room temperature and  
 129 pH was regulated to neutral. Precipitates were separated us-  
 130 ing an adsorbent magnet, washed three times with ethanol  
 131 and deoxygenated distilled water, respectively and then finally  
 132 dried in an oven at 60 °C. Dried precipitates were powdered  
 133 to obtain magnetic *Rhizopus oryzae* biomass particles.

134 **Characterization of magnetic *Rhizopus oryzae* biom-**  
 135 **ass particles:** Wide-angle X-ray diffraction (XRD) measure-  
 136 ments were carried out on an XRD diffractometer (D8-Ad-  
 137 vance, Bruker, USA). Samples were cut into powders in order  
 138 to eliminate the influence from crystalline orientation. Pat-  
 139 terns were obtained with CuK<sub>α</sub> radiation (λ = 0.15406 nm) at  
 140 40 kV and 40 mA and recorded in the region of 2θ from 10 to  
 141 70° with a step speed of 2° min<sup>-1</sup>. *R. oryzae* biomass and mag-  
 142 netic *Rhizopus oryzae* biomass particles surfaces were exam-  
 143 ined by SEM (Hitachi S4300). Materials were coated with  
 144 platinum under vacuum conditions before the SEM experi-  
 145 ments. The FT-IR spectra of the native and congo red laden  
 146 magnetic *Rhizopus oryzae* biomass particles were obtained  
 147 using a Thermo Nicolet NEXUS TM spectrophotometer. All  
 148 samples were prepared as potassium bromide pellets.

149 **Adsorption experiments:** All batch adsorption experi-  
 150 ments were performed on a shaking thermostat (KYC-1102C,  
 151 Ningbo, China) with a constant speed of 100 rpm. Typically,  
 152 50 mL of a dye solution of a desired concentration and mag-  
 153 netic *Rhizopus oryzae* biomass particles with a desired dos-  
 154 age were added into 250 mL conical glass flasks with a con-  
 155 stant speed of 100 rpm at 298 K. After the completion of pre-  
 156 set time intervals, 5 mL of the dispersion was drawn and sepa-  
 157 rated immediately using an adsorbent magnet to collect the  
 158 bioadsorbent. The residual congo red concentration in the  
 159 supernate was analyzed at λ<sub>max</sub> = 496 nm using a Cary 50 model  
 160 UV-visible spectrophotometer (Varian, USA). The concentration  
 161 retained in the adsorbent phase (q<sub>t</sub>, mg/g) and color removal effi-  
 162 ciency (η, %) were calculated using eqns. 1-2, respectively.

$$q_t = \frac{(C_0 - C_t)V}{W} \quad (1) \quad 163$$

$$\eta(\%) = \frac{(C_0 - C_t)}{C_0} \times 100\% \quad (2) \quad 164$$

where  $C_0$ (mg/L) is the initial congo red concentration and  $C_t$  (mg/L) is the congo red concentration at time  $t$  (min),  $V$  (l) is the volume of solution and  $W$  (g) is the bioadsorbent weight.

## RESULTS AND DISCUSSION

**XRD analysis:** Fig. 2 shows the XRD patterns of (a) the *R. oryzae* biomass, (b)  $Fe_3O_4$  and (c) the magnetic *Rhizopus oryzae* biomass particles. The wide and irregular peak illustrated that the *R. oryzae* biomass is not a single crystal structure, but of mixed composition. The main peak at  $2\theta = 19.73^\circ$  is assigned to the (110) planes similar to that of chitin and its derivatives. Thus, chitin may be the main component of *R. oryzae* biomass<sup>14,15,32</sup>. The main peaks of  $Fe_3O_4$  were at 30.32, 35.64, 43.36, 53.67, 57.26 and 62.87°, respectively corresponded to the (2 2 0), (3 1 1), (4 0 0), (4 2 2), (5 1 1) and (4 4 0) crystal planes of pure  $Fe_3O_4$  with a spinal structure<sup>28</sup>. In the XRD pattern of the magnetic *Rhizopus oryzae* biomass particles, six obvious diffraction peaks of (2 2 0), (3 1 1), (4 0 0), (4 2 2), (5 1 1) and (4 4 0) were observed, indicating the introduction of  $Fe_3O_4$  with a spinal structure into the magnetic *Rhizopus oryzae* biomass particles surfaces. The diffraction peak of *R. oryzae* at  $2\theta = 19.73^\circ$  could not be found in XRD pattern of the magnetic *Rhizopus oryzae* biomass particles, indicating that a change in the structure of chitin occurred preparation.

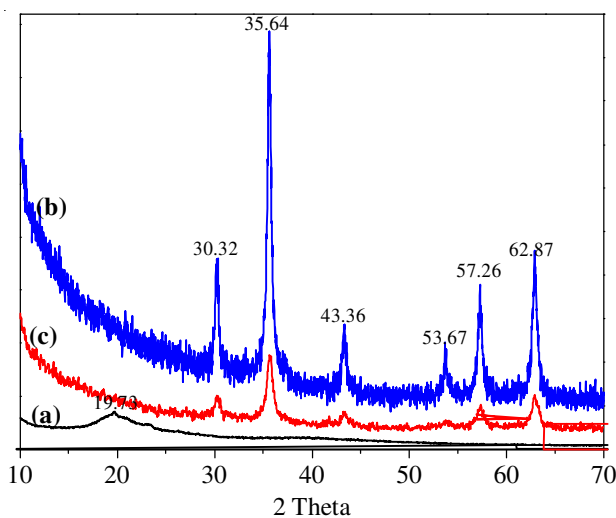


Fig.2. X-ray powder diffraction patterns for (a) *R. oryzae* biomass, (b)  $Fe_3O_4$  and (c) magnetic *Rhizopus oryzae* biomass particles

**SEM analysis:** SEM is used extensively as a tool for biosorbent characterization<sup>33</sup>. A comparison between the SEM images of the *R. oryzae* biomass and those of the magnetic *Rhizopus oryzae* biomass particles is illustrated in Fig. 3. The surface morphology of pristine *R. oryzae* biomass is conspicuously different from that of the magnetic *Rhizopus oryzae* biomass particles. Magnified images of *R. oryzae* biomass show a smooth and homogeneous surface morphology (Fig. 3a,b). No obvious pores and voids were found on the *R. oryzae* biomass surface, indicating it's relatively dense. In contrast, magnetic *Rhizopus oryzae* biomass particles surface clearly turned rough and irregular when  $Fe_3O_4$  particles were attached to them (Fig. 3c,d). Obviously, the uneven surface of the magnetic

*Rhizopus oryzae* biomass particles indicated active adsorption sites and provides an advantageous condition for attracting more target pollutants around the sites. Thus, improved adsorption rates and capacities could be expected from the magnetic *Rhizopus oryzae* biomass particles<sup>34</sup>.

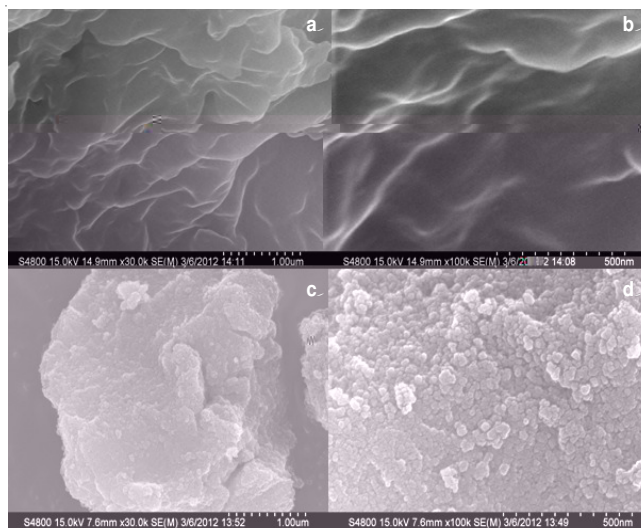


Fig. 3. SEM images for (a-b) *R. oryzae* biomass particle and (c-d) magnetic *Rhizopus oryzae* biomass particles

**Magnetic recovery of magnetic *Rhizopus oryzae* biomass particles:** The prepared magnetic *Rhizopus oryzae* biomass particles could be readily dispersed in water under stirring (Fig. 4a).

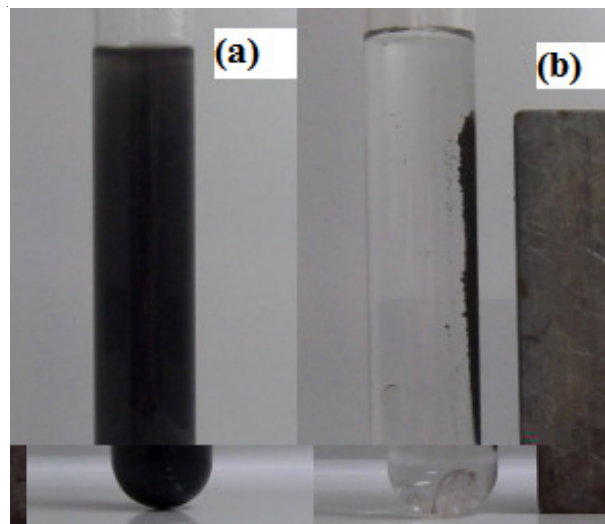


Fig. 4. Photographs of (a) magnetic *Rhizopus oryzae* biomass particles dispersed in treated water solution and (b) magnetic *Rhizopus oryzae* biomass particles by an ordinary magnet after 5 s

Moreover,

$$34.2ic R. -0.010 Tc 1-2.0 0 Td (,ed)T -0.000$$

**FT-IR analysis:** The FT-IR spectra of magnetic *Rhizopus oryzae* biomass particles before and after congo red biosorption were taken from 4000-400  $\text{cm}^{-1}$  to identify active functional groups during biosorption as shown in Fig. 5.

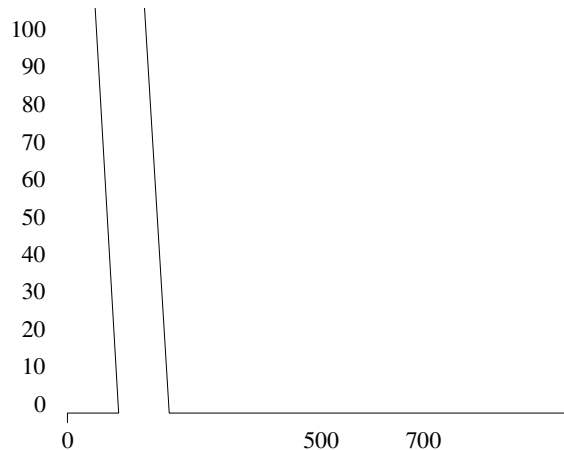
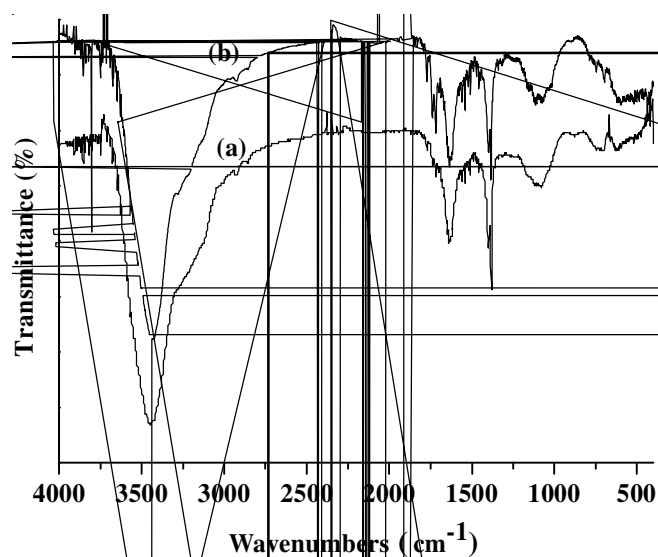


Fig. 5. FT-IR spectra of magnetic *Rhizopus oryzae* biomass particles: (a) before congo red biosorption; (b) after congo red biosorption

reflected N-H and O-H stretching vibrations of hydroxyl and amine groups on the surface of the magnetic *Rhizopus oryzae* biomass particles. The band at 3450  $\text{cm}^{-1}$  could be ascribed to the carboxyl groups. A strong band at 3300  $\text{cm}^{-1}$  reflected N-H and O-H stretching vibrations of hydroxyl and amine groups on the surface of the magnetic *Rhizopus oryzae* biomass particles. The band at 2930  $\text{cm}^{-1}$  could be ascribed to the carboxyl groups. A distinct band at 1728  $\text{cm}^{-1}$  resulted from the vibrations of the CO and CN (amide I) peptidic bonds. The signal located near 1640  $\text{cm}^{-1}$  could be ascribed to the carboxyl groups. A strong band at 1580  $\text{cm}^{-1}$  corresponds to the C-O bond, which is the characteristic peak of amides<sup>35-37</sup>. The intensities at 1640 (amide I) and 1384  $\text{cm}^{-1}$  (amide II) bands nearly decreased after congo red biosorption, suggesting the interaction between congo red and the amine groups on the surface of the magnetic *Rhizopus oryzae* biomass particles. After loading magnetic *Rhizopus oryzae* biomass particles with congo red, the band intensities at 1384  $\text{cm}^{-1}$  (amide II) and 1080  $\text{cm}^{-1}$  (amide III) bands also shifted to 602 and 800  $\text{cm}^{-1}$ , respectively. These changes in band intensities, addition, and shift suggest the involvement of NH and OH of hydroxyl groups, the  $\text{CH}_2$  group of lipids, carboxyl groups, and the CO group of polysaccharides on magnetic *Rhizopus oryzae* biomass particles.

#### Magnetic *Rhizopus oryzae* biomass particles

The adsorption capacity of *Rhizopus oryzae* biomass particles for congo red removal from aqueous solution was studied. Various magnetic *Rhizopus oryzae* biomass particles were prepared from 0.6 to 3.0  $\text{g L}^{-1}$  at a fixed congo red concentration of 10  $\text{mg L}^{-1}$ . The result is shown in

64.1 % removal were observed within 2 h and the final color removal was found to be as high as 99.8, 97.1 and 95.5 % within 5, 12 and 13 h, respectively. As the congo red initial concentration increased (50-80 mg L<sup>-1</sup>), the color removal efficiency of congo red solution onto magnetic *Rhizopus oryzae* biomass particles by adsorption slowly increased until equilibrium was attained. Only 40.8 and 27.1 % adsorption was observed within 2 h whereas the final color removal efficiencies were found to be 94.1 and 79.8 % within 28 and 31 h, respectively. Although the final color removal efficiency at initial congo red concentrations of 20 and 50 mg L<sup>-1</sup> showed no significant differences, the equilibrium time between the solutions differed by 25 h. These results may be explained by the following: A large number of vacant surface sites are available for adsorption during the initial stage of adsorption or under low initial congo red concentration. With increasing adsorption time, the remaining vacant surface sites became difficult to occupy due to repulsive forces between the congo red dye adsorbed on the surface of the magnetic *Rhizopus oryzae* biomass particles and solution phase<sup>40</sup>. The amount of congo red adsorbed per unit weight of magnetic *Rhizopus oryzae* biomass particles at equilibrium increased with increasing initial congo red concentration. As the initial concentration increased from 5 to 80 mg L<sup>-1</sup>, the equilibrium adsorption capacity increased from 6.32 to 65.19 mg g<sup>-1</sup>. Therefore, the adsorption process is highly dependent on the initial congo red concentration and contact time.

**Adsorption kinetics:** To further expose the adsorption mechanism of congo red onto magnetic *Rhizopus oryzae* biomass particles rate-controlling steps, a kinetic investigation was conducted. The Lagergren-first-order, pseudo-second-order and intra-particle diffusion kinetic models were applied to model the kinetics of congo red adsorption onto magnetic *Rhizopus oryzae* biomass particles.

Lagergren-first-order kinetic model<sup>41</sup> is generally expressed as:

$$\log (q_e - q_t) = \log q_e - \frac{k_1 t}{2.303} \quad (3)$$

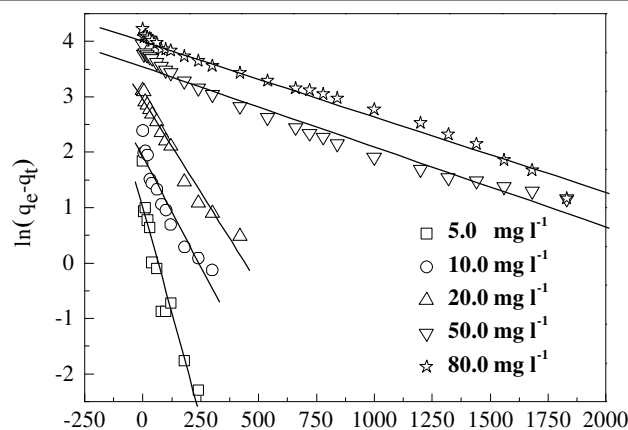
where  $q_e$  and  $q_t$  are amounts of congo red (mg g<sup>-1</sup>) adsorbed on the adsorbent at equilibrium and at a given time  $t$ , respectively and  $k_1$  is the rate constant (min<sup>-1</sup>) of the adsorption model, the value of which can be calculated from plots of  $\log (q_e - q_t)$  versus  $t$  as in eqn. 3.

The pseudo-second-order kinetic model<sup>42</sup> proposed by Ho and McKay is expressed as follows:

$$\frac{t}{q_t} = \frac{1}{k_2 q_e^2} + \frac{t}{q_e} \quad (4)$$

where  $k_2$  is the rate constant (g mg<sup>-1</sup> min<sup>-1</sup>) of the pseudo-second-order kinetic model of adsorption. By plotting a curve of  $t/q_t$  against  $t$ ,  $q_e$  and  $k_2$  can be evaluated. The adsorption parameters were determined at different initial congo red concentrations. Results are presented in Fig. 8a,b and Table-1.

In all studied initial congo red concentrations, extremely high correlation coefficients (>0.991) were obtained from calculations using the pseudo-second order kinetic equation. In addition, calculated  $q_e$  values were also in agreement with the experimental data in the case of pseudo-second-order kinetics





For example, chitin has two main functional groups, the hydroxyl and amino groups, per glucosamine unit. Therefore, the dye could be adsorbed by interaction between the congo red dye molecules and the functional groups of chitin in magnetic *Rhizopus oryzae* biomass particles at low congo red concentrations. The Lagergren-first-order kinetic model indicates that the rate of occupation of biosorption sites is proportional to the number of unoccupied sites. Congo red dye molecules compete with each other for the active surface sites of magnetic *Rhizopus oryzae* biomass particles at high congo red concentrations (80.0 mg L<sup>-1</sup>) and the chemical interaction involving valence forces between the adsorbent and sorbate became is weakened<sup>20,34</sup>.

To assess the nature of the diffusion process, kinetic data were analyzed using an intra-particle diffusion model<sup>25</sup> to elucidate the diffusion mechanism:

$$q_t = k_i t^{1/2} + c \quad (5)$$

where  $c$  (mg g<sup>-1</sup>) is the intercept and  $k_i$  is the intra-particle diffusion rate constant (mg g<sup>-1</sup> min<sup>-1/2</sup>). The value of  $k_i$  can be calculated from the slope of linear plots of  $q_t$  versus  $t^{1/2}$ .

Prediction of the rate-limiting step in an adsorption process is very important to understand the sorption mechanism of the particles. According to this model, if the plot of  $q_t$  versus  $t^{1/2}$  gives a straight line, then the adsorption process is controlled by intra-particle diffusion. If the data exhibit multi-linear plots, then two or more steps influence the adsorption process<sup>35</sup>. All of the correlation coefficients for the intra-particle diffusion model were lower than those of the pseudo-first-order and the pseudo-second-order models when the congo red concentration was within 5 to 50 mg L<sup>-1</sup>, as shown in Fig. 8c and Table-2.

This result indicates that congo red adsorption onto magnetic *Rhizopus oryzae* biomass particles does not follow the intra-particle diffusion kinetics. Plots of  $q_t$  versus  $t^{1/2}$  can be divided into a multi-linearity correlation (Fig. 8c), indicating the occurrence of three steps during adsorption process at low congo red concentration. Congo red in aqueous solution is

first transported onto the surface of magnetic *Rhizopus oryzae* biomass particles (film diffusion). The second step is the gradual adsorption stage, where intra-particle diffusion with  $k_2$  (0.053, 0.144, 0.765 and 1.515 mg g<sup>-1</sup> min<sup>-1/2</sup> for 5, 10, 20 and 50 mg L<sup>-1</sup>, respectively) can be rate-controlling. The third step is the final equilibrium stage, where intra-particle diffusion starts to slow down due to the extremely low solute concentration in the solution. In the intermediate stage, where adsorption is gradual, the process may be controlled by intra-particle diffusion, indicating that intra-particle diffusion is involved in congo red adsorption onto magnetic *Rhizopus oryzae* biomass particles, but is not the sole rate-controlling-step. The plot of  $q_t$  versus  $t^{1/2}$  gives a straight line at increased congo red concentration (80 mg L<sup>-1</sup>), indicating that the adsorption process is only controlled by intra-particle diffusion. From the above analysis, film diffusion and intra-particle diffusion simultaneously operate during congo red adsorption on magnetic *Rhizopus oryzae* biomass particles at low concentration (5-50 mg L<sup>-1</sup>) and are enhanced with increasing initial congo red concentration. Intra-particle diffusion is the sole rate-limiting step at high congo red concentration (80 mg L<sup>-1</sup>).

**Equilibrium adsorption isotherm:** The Langmuir and Freundlich isotherm models were used to describe the equilibrium adsorption of congo red on magnetic *Rhizopus oryzae* biomass particles. Linear forms of the Langmuir equation<sup>43</sup> eqn. 6 and Freundlich isotherm<sup>44</sup> eqn. 7 after rearrangement are as follows:

$$\text{Ln}q_e = \text{Ln}K_F + \frac{1}{n} \text{Ln}C_e \quad (6)$$

$$\frac{C_e}{q_e} = \frac{C_e}{q_m} + \frac{1}{K_L q_m} \quad (7)$$

where  $q_e$  (mg g<sup>-1</sup>) is the adsorption capacity of congo red adsorbed at equilibrium,  $C_e$ (mg L<sup>-1</sup>) is the equilibrium concentration of congo red in solution.  $q_m$ (mg g<sup>-1</sup>) is the maximum amounts of congo red adsorbed per unit weight of adsorbent required for monolayer coverage of the surface,  $K_L$ (L

TABLE-1  
A COMPARISON OF LAGERGREN-FIRST-ORDER MODEL AND  
PSEUDO-SECOND-ORDER MODEL RATE CONSTANTS CALCULATED FROM EXPERIMENTAL DATA

C <sub>0</sub> (mg l <sup>-1</sup> )	q <sub>e,exp</sub> (mg g <sup>-1</sup> )	Lagergren-first-order kinetic model			Pseudo-second-order kinetic model		
		q <sub>e,cal</sub> (mg g <sup>-1</sup> )	k <sub>1</sub> (min <sup>-1</sup> )	R <sup>2</sup>	q <sub>e,cal</sub> (mg g <sup>-1</sup> )	K <sub>2</sub> (min <sup>-1</sup> )	R <sup>2</sup>
5.0	6.32	2.79	0.0357	0.950	6.31	0.02562	1.000
10.0	10.88	6.86	0.0183	0.954	10.92	0.00382	1.000
20.0	21.75	19.12	0.0154	0.982	22.71	0.00070	0.999
50.0	49.13	43.05	0.0035	0.984	52.22	0.00013	0.997
80.0	65.19	63.92	0.0033	0.996	68.31	0.00006	0.991

TABLE-2  
INTRA-PARTICLE DIFFUSION MODEL FOR CONGO RED ADSORPTION ON  
MAGNETIC *Rhizopus oryzae* BIOMASS PARTICLES FOR DIFFERENT INITIAL CONCENTRATIONS

C <sub>0</sub> (mg l <sup>-1</sup> )	Whole process			First stage			Second stage	Third stage
	C (mg g <sup>-1</sup> )	k <sub>i</sub> (mg g <sup>-1</sup> min <sup>-0.5</sup> )	R <sup>2</sup>	C <sub>1</sub> (mg g <sup>-1</sup> )	K <sub>1</sub> (mg g <sup>-1</sup> min <sup>-0.5</sup> )	R <sub>1</sub> <sup>2</sup>	C <sub>2</sub> (mg g <sup>-1</sup> )	

412  $\text{mg}^{-1}$ ) is a constant related to the heat of adsorption.  $K_F(\text{mg}^{-1}$   
 413  $^{(1/n)}\text{L}^{1/n}\text{g}^{-1}$ ) is related to the adsorption capacity of the adsor-  
 414 bent and  $1/n$  is another constant related to the surface  
 415 heterogeneity. The theoretical parameters ( $q_m$ ,  $K_L$ ,  $K_F$  and  $n$  and  
 416  $R^2$ ) of the adsorption isotherms are summarized in Table-3.

TABLE-3  
 ISOTHERM MODELS CONSTANTS AND REGRESSION  
 COEFFICIENTS FOR CONGO RED ADSORPTION ONTO  
 MAGNETIC *Rhizopus oryzae* BIOMASS PARTICLES

T(K)	Langmuir isotherm constants			Freundlich isotherm constants		
	$q_m$ ( $\text{mg g}^{-1}$ )	$K_L$	$R^2$	$K_F$ ( $\text{mg}^{-1(1/n)}\text{L}^{1/n}\text{g}^{-1}$ )	$n$	$R^2$
298	69.78	0.85	0.994	24.78	2.92	0.955

417 Congo red adsorption on magnetic *Rhizopus oryzae* bio-  
 418 mass particles fits the Langmuir model ( $R^2 = 0.994$ ) better than  
 419 the Freundlich model ( $R^2 = 0.955$ ) under the concentration  
 420 range studied due to the homogeneous distribution of active  
 421 sites on the magnetic *Rhizopus oryzae* biomass particles sur-  
 422 face, since the Langmuir equation assumes a homogenous  
 423 surface. As seen in Table-3, the maximum adsorption capaci-  
 424 ty of congo red onto magnetic *Rhizopus oryzae* biomass par-  
 425 ticles is  $69.78 \text{ mg g}^{-1}$ , consistent with the experimentally ob-  
 426 tained value and indicating a monolayer adsorption process.

#### 427 Conclusion

428 In this study, magnetic *Rhizopus oryzae* biomass particles  
 429 were synthesized and characterized as a novel adsorbent for  
 430 the removal of typical azo dye (CR) from aqueous solution.  
 431 The adsorbent dose, initial congo red concentration and con-  
 432 tact time during adsorption played significant roles in the dye  
 433 adsorption capacity of magnetic *Rhizopus oryzae* biomass par-  
 434 ticles. In the kinetic study, the pseudo-second order kinetic  
 435 model described the process of congo red adsorption on mag-  
 436 netic *Rhizopus oryzae* biomass particles at low congo red con-  
 437 centration ( $5\text{-}50 \text{ mg L}^{-1}$ ) very well. Adsorption kinetic studies  
 438 also revealed that three stages in the adsorption process. Both  
 439 film diffusion and intra-particle diffusion simultaneously op-  
 440 erated during adsorption at low congo red concentrations ( $5\text{-}$   
 441  $50 \text{ mg L}^{-1}$ ). Intra-particle diffusion is the sole rate-limiting step  
 442 at high congo red concentration ( $80 \text{ mg L}^{-1}$ ). Isotherm model-  
 443 ing revealed that the Langmuir equation could better describe  
 444 congo red adsorption on magnetic *Rhizopus oryzae* biomass  
 445 particles compared with Freundlich models. Batch adsorption  
 446 experiments showed that magnetic *Rhizopus oryzae* biomass  
 447 particles may have broad applications in the removal of an-  
 448 ionic azo dyes from wastewater and that it can be competitive  
 449 with conventional adsorbents. Other studies on this  
 450 bioadsorbent continue in our laboratory and more detailed  
 451 results will appear in a forthcoming paper.

#### ACKNOWLEDGEMENTS

452 This work was financially supported by the National Natu-  
 453 ral Science Foundation of China (Grant Nos. 21106091.  
 454 51208331) and Zhejiang Provincial Natural Science Founda-  
 455 tion of China (LQ12B06004).

#### REFERENCE

1. G. Crini, *Bioresour. Technol.*, **97**, 1061 (2006).
2. H. Park and W. Choi, *J. Photochem. Photobiol. Chem.*, **159**, 241 (2003).
3. R. Gong, Y. Ding, M. Li, C. Yang, H. Liu and Y. Sun, *Dyes Pigments*, **64**, 187 (2005).
4. K.C. Chen, J.Y. Wu, C.C. Huang, Y.M. Liang and S.C.J. Hwang, *J. Biotechnol.*, **101**, 241 (2003).
5. M.S. Chiou and G.S. Chuang, *Chemosphere*, **62**, 731 (2006).
6. S. Chinwetkitvanich, M. Tuntoolvest and T. Panswad, *Water Res.*, **34**, 2223 (2000).
7. U. Mayer, *FEMS Symp.*, **12**, 371-385 (1981).
8. K.T. Chung and C.E. Cerniglia, *Mutat. Res.*, **277**, 201 (1992).
9. G. Ciardelli, L. Corsi and M. Marcucci, *Resour. Conserv. Recycling*, **31**, 189 (2001).
10. K. Swaminathan, S. Sandhya, A. Carmalin Sophia, K. Pachhade and Y.V. Subrahmanyam, *Chemosphere*, **50**, 619 (2003).
11. I.D. Mall, V.C. Srivastava, N.K. Agarwal and I.M. Mishra, *Chemosphere*, **61**, 492 (2005).
12. C. Namasivayam and D.J.S.E. Arasi, *Chemosphere*, **34**, 401 (1997).
13. L. Wang and A.Q. Wang, *J. Chem. Technol. Biotechnol.*, **82**, 711 (2007).
14. P.R. Austin, C.J. Brine, J.E. Castle and J.P. Zikakis, *Science*, **212**, 749 (1981).
15. M.K. Jang, B.G. Kong, Y.I. Jeong, C.H. Lee and J